AWARD NUMBER: W81XWH-20-1-0269

TITLE: Detection and Treatment of Ovarian Cancer by Targeting Tumor Extracellular Hydroxyapatite: A New Paradigm

PRINCIPAL INVESTIGATOR: Mohammed Noor Tantawy

CONTRACTING ORGANIZATION: Vanderbilt University Medical Center, Nashville, TN

REPORT DATE: May 2022

TYPE OF REPORT: Annual

PREPARED FOR: U.S. Army Medical Research and Development Command

Fort Detrick, Maryland 21702-5012

REPORT DOCUMENTATION PAGE	*Form Approved* *OMB No. 0704-0188*

Public reporting burden for this collection of information is estimated to average 1 hour per response, including the time for reviewing instructions, searching existing data sources, gathering and maintaining the data needed, and completing and reviewing this collection of information. Send comments regarding this burden estimate or any other aspect of this collection of information, including suggestions for reducing this burden to Department of Defense, Washington Headquarters Services, Directorate for Information Operations and Reports (0704-0188), 1215 Jefferson Davis Highway, Suite 1204, Arlington, VA 22202-4302. Respondents should be aware that notwithstanding any other provision of law, no person shall be subject to any penalty for failing to comply with a collection of information if it does not display a currently valid OMB control number. **PLEASE DO NOT RETURN YOUR FORM TO THE ABOVE ADDRESS.**

1. REPORT DATE: May 2022	**2. REPORT TYPE: Annual**	**3. DATES COVERED:** 01May2021-30Apr2022

4. TITLE AND SUBTITLE Detection and Treatment of Ovarian Cancer by Targeting Tumor Extracellular Hydroxyapatite: A New Paradigm	**5a. CONTRACT NUMBER:** **5b. GRANT NUMBER: W81XWH-20-1-0269** **5c. PROGRAM ELEMENT**
6. AUTHOR(S): Mohammed N Tantawy and J. Oliver McIntyre	**5d. PROJECT NUMBER** **5e. TASK NUMBER** **5f. WORK UNIT NUMBER**
7. PERFORMING ORGANIZATION NAME(S) AND ADDRESS(ES) Vanderbilt University Medical Center 1161 21st Ave South Nashville TN 37232	**8. PERFORMING**
9. SPONSORING / MONITORING AGENCY NAME(S) AND ADDRESS(ES) U.S. Army Medical Research and Development Command Fort Detrick, Maryland 21702-5012	**10. SPONSOR/MONITOR'S ACRONYM(S)** **11. SPONSOR/MONITOR'S NUMBER(S)**

12. DISTRIBUTION / AVAILABILITY STATEMENT

Approved for Public Release; Distribution Unlimited

13. SUPPLEMENTARY NOTES

14. ABSTRACT

Introduction: In this report, we continue to evaluate tumor extracellular hydroxyapatite (HAP), $Ca_{10}(PO_4)_6OH_2$, as an imaging biomarker of ovarian cancer a target for therapy. We have shown that HAP-binding radiotracers such as FDA-approved ^{18}F-NaF can be used with PET imaging and ^{99m}Tc-MDP with SPECT imaging to detect breast tumors; in this context, detection of tumor-associated HAP exhibited high specificity and a high signal-to-background ratio (SBR) as HAP is absent in normal soft tissue. In ovarian cancer, conventional imaging modalities lack clear metrics for assessing tumor burden before and after surgical debulking and for assessing tumor response to therapy. This is mainly due to lack of specificity and/or low SBR ratio from standard imaging. Additionally, we had developed a nanoparticulate sulfonated polystyrene solution (NSPS) to break-up HAP *in vivo* inducing a localized alkalosis status in the tumor microenvironment inhibiting tumor growth.

Methods: Ovarian tumor cells that constitutively express a luciferase reporter (ID8-luc) were cultured in normal media and in osteogenic media to help increase chances of HAP production. Cells were treated with NSPS in triplicates and dead cells to total cells were counted. For *in vivo* studies, female C57Bl/6 mice received intraperitoneal injection of ID8-luc (10^6). After four weeks, bioluminescence imaging (BLI) was used to assess tumor burden and the mice were injected with ~11 MBq/0.1 mL of ^{18}F-NaF and imaged 60 min later for 20 min in a microPET/CT. Within 24 hours, the mice were injected with ~37 MBq/0.1 mL of ^{99m}Tc-MDP and imaging 60 min later in a NanoSPECT/CT for about 20 min. The imaging protocols were repeated weakly. When tumor burden was detected across the different modalities, the mice were treated with weekly 2 mg/kg cisplatin, 100 mg/kg NSPS (one time), or vehicle, PBS, weekly (controls). After several weeks of cisplatin treatment, some of the mice were taken off cisplatin and treated with PBS as a model for tumor recurrence. Regions of interest (ROIs) were drawn around the abdominal cavity and retention of ^{18}F-NaF within the ROI was estimated. Furthermore, NSPS impact on tumors was assessed via IHC in harvested tumors. In addition, tumor extracellular HAP was assessed in clinically annotated tissue microarray (TMA) of patient samples from the Vanderbilt University Medical Center (VUMC) Tissue Repository for Ovarian Cancer (TROC). Correlations between HAP and tumor characteristics were investigated.

Results: We found increased ID8 tumor cell death in the osteogenic media compared to normal media potentially indicating that the impact of NSPS on tumor cells is proportional to extracellular HAP abundance. Due to the absence of HAP in normal soft tissue, peritoneal ovarian tumors were detected with high specificity and SBR using ^{18}F-NaF PET which corresponded with BLI and pathology. We demonstrate that imaging tumor-extracellular HAP provided a suitable marker for tracking tumor response to therapy. Retention of ^{18}F-NaF was reduced in the cisplatin and NSPS treated mice indicating tumor regression but increased in the PBS treated mice indicating tumor progression. Increase ^{18}F-NaF uptake was observed later in the cisplatin then PBS treated mice indicating that tumor extracellular HAP can also be an indicator of tumor recurrence. Due to the retention of ^{99m}Tc-MDP in the liver, we could not reliably identify tumor burden using ^{99m}Tc-MDP SPECT imaging. NSPS was also found to inhibit tumor metabolism as determined by reduced ^{18}F-FDG uptake in tumors. Additionally, NSPS was found to prolong mouse models of ovarian cancer by more than 47%. Among 163 cases from the VUMC TROC, HAP staining was more common among serous than non-serous and disease remission took less years when extracellular HAP was present than tumors without HAP.

15. SUBJECT TERMS

None listed.

16. SECURITY CLASSIFICATION OF:			**17. LIMITATION**	**18. NUMBER OF PAGES**	**19a. NAME OF RESPONSIBLE PERSON**
a. REPORT	**b. ABSTRACT**	**c. THIS PAGE**			USAMRDC
Unclassified	Unclassified	Unclassified	Unclassified	21	**19b. TELEPHONE NUMBER** *(include area code)*

Table of Contents

1. **Introduction**

Hydroxyapatite (HAP), $Ca_{10}(PO_4)_6OH_2$, once thought to be solely an ubiquitous component of bone, has also been shown to be produced by some types of malignancies via a classical mechanism; alkaline phosphates (ALP) on the surface of cells hydrolyses beta-glycerophosphate (□G) to glycerol and inorganic phosphate (Pi). Pi then combines with calcium in the cell to produce HAP crystals, and then this HAP is deposited in the extracellular space contributing to the structural matrix that influences the tumor microenvironment (1-9). Capitalizing on the presence of extracellular HAP and our expertise in imaging, we have shown that HAP-binding targeting radiotracers - such as FDA-approved ^{18}F-labeled sodium fluoride (^{18}F-NaF) and ^{99m}Tc-labeled methyl diphosphate (^{99m}Tc-MDP) can be used with positron emission tomography (PET) and single photon emission computer tomography (SPECT), respectively, to detect breast tumors; detection of tumor-associated HAP exhibited high specificity and a high signal-to-background ratio (SBR) as HAP is absent in normal soft tissue (10, 11). Furthermore, we had developed a nanoparticulate sulfonated polystyrene solution (NSPS) designed to chelate calcium and subsequently break up tumor extracellular HAP into its basic components, $Ca^{++} + PO_4^{-} + OH^{-}$. Dissolution of HAP is predicted to release phosphate and hydroxyl ions in the tumor extracellular milieu inducing a localized microenvironment alkalosis (high pH). Therefore, in this proposal we aimed at testing the hypothesis that tumor extracellular hydroxyapatite is viable target for detecting and treating ovarian cancer. We proposed a battery of *in vitro* and *in* vivo studies to test this hypotheses.

2. **Keywords**

Hydroxyapatite, ^{18}F-NaF, ^{99m}Tc-MDP, PET, SPECT, ID8-luc, HGSOC, ovarian cancer.

3. **Accomplishments**

A. Major goals and accomplishments

Research-Specific Tasks:

Specific Aim 1: Investigate the efficacy of NSPS in ovarian cancer	Months	Investigator	% Accomplished
•Submission of institution approved animal protocols and related material for DoD's ACURO approval. •Received ACURO approval before initiating animal experiments.		Dr. Tantawy	100% completed
Major Task 1: Treatment with NSPS			
Subtask 1: Cell culture <u>Cell lines.</u> **ID8 mouse ovarian cancer cells** were obtained directly from their academic source (Dr. Kathy Roby, Dr. Iain McNeish and Dr. Sandra Orsulic, respectively). We have used this cell line and verified the presence of tumor extracellular hydroxyapatite. 3D culture as tumor spheroids will be established and cell viability following treatmetn with NSPS versus vehicle (PBS) will be measured using a commercially available Cultrex Spheroid Colorimetric Assay	1-6	Dr. Tantawy Dr. Wilson Dr. McIntyre RA	95% completed: Cell culture for injection in mice. Cell viability completed. Need to make non-buffered media to accurately measure acidity.

Subtask 2: Intraperitoneal (i.p.) injection of ID8-luc cells into C57Bl/6	1-7	Dr. Wilson Dr. Yull	90% completed
Subtask 3: Treat mice with a one-time i.p. bolus injection of NSPS. Euthanize and harvest tissue at 0.25, 0.5, 1, 2, 4, 7 and 24 hours (n = 3 per time point) for pharmacokinetic (PK) analysis. Ntot = 21 mice	2-12	Dr. Tantawy RA	60% completed. Need to thaw frozen tissue and grind to complete task
Subtask 4: Repeat subtasks 2 and 3 and treat with one time NSPS i.p injection but euthanize and harvest tissue at 7, 14, 21, and 28 days post NSPS (n = 3 per time point) for assessment of tumor growth. Analyze the results statistically. Ntot = 12 mice	13-21	Dr. Tantawy Dr. Wilson RA	60% completed. Need to thaw frozen tissue and grind to complete task
Subtask 5: LS/MS/MS and pharmacokinetic analysis. Statistical analysis	6-21	Dr. Tantawy Dr. Rook Dr. Beeghly-Fadiel Dr. McIntyre	5%. NSPS does not pass through LS column. May have to do MS only. Carrying out test to see if MS alone is sufficient.
Milestone(s) Achieved: NSPS efficacy verified both in vitro as demonstrated by lower cell colonies compared to controls and in vivo via pathology and histology Establish pharmacokinetic parameters. Publish results in peer review journal.			
Specific Aim 2: HAP imaging in mouse models of ovarian cancer			
Major Task 2: Mouse models and imaging			
Subtask 1: Inject ID8-luc cells into C57Bl/6 mice, i.p. (n = 30)	1-3	Dr. Wilson Dr. Yull	99% Progress here has been slow due to COVID19 lockdown
Subtask 2: One week later, the Center for Small Animal Imaging (CSAI) at Vanderbilt Medical Center will image the mice weekly for 3 weeks with ^{18}F-NaF PET, ^{99m}Tc-MDP SPECT, and bioluminescence.	2-4	CSAI	99%
Subtask 2: At 4 weeks post ID8-luc injection, administer 5 mg/kg cisplatin (intravenous) weekly for 4 weeks (n = 10) or NSPS (i.p.) once (n = 10) or vehicle (PBS) once, i.p. (n = 10). Maintain	3-8	Dr. Tantawy Dr. Wilson	99%

weekly imaging for 4 more weeks		CSAI	
Subtask 3: Draw regions-of-interest around tumors, establish time-activity curves and then carry out statistical analyses comparing each time point to the previous time point and comparing cisplatin treatment results to NSPS treatment results.	3-18	Dr. Tantawy Dr. Beeghly-Fadiel	99%
Milestone(s) Achieved: Tumor extracellular HAP imaging can be used to detect tumor burden, tumor distribution, tumor progression, and tumor regression following cisplatin and NSPS treatments. Publish results in peer review journal.			
Specific Aim 3: Elucidate correlations between extracellular HAP in tumors and clinically relevant indicators in ovarian cancer patients			
•Submission of institution's IRB approval and related material for DoD's HRPO approval. •Received HRPO approval or exempt finding, before initiating human subjects/HAS related studies.		Dr. Tantawy	100%
Major Task 3: Send ovarian tissue microarrays (TMAs) to Vanderbilt's Translational Pathology Shared Resources (TPSR) for sectioning and staining.			
Subtask 1: Stain with alizarin red S and von Kossa	1-6	TPSR	100%
Subtask 2: Unstained sections loaded onto calcium fluoride slides will be imaged via Raman spectroscopy by CSAI.	2-12	CSAI	99%. Raman may not be feasible for samples that have less than 1% HAP compared to sample size.
Subtask 3: Digital images (40x) of the stained slides will be carried out by the Digital Histology Shared Resources (DHSR) at Vanderbilt Medical Center.	1-6	DHSR	100%
Subtask 3: Determine which sections scored positive for alizarin red S and con Kossa and if a 960 cm^{-1} Raman shift was detected. Correlate results with clinically relevant indicators.	1-21	Dr. Tantawy Dr. Watkins Dr. Crispens Dr. Beeghly-Fadiel	90% Thorough statistical analysis in progress
Milestone(s) Achieved: Tumor extracellular HAP is correlated with patient survival rate, chemotherapy sensitivity, and other clinically relevant metrics that reinforce the need to image patients with HAP-targeting radioligands to better inform physicians and improve patient management. Publish results in peer review journal.			

B. Significant results and key outcomes.

We stained 163 formalin-fixed paraffin-embedded human ovarian carcinomas in tissue microarrays (TMAs) with von Kossa (for phosphates) and alizarin red S (for calcium), see **Figure 1.** Additionally, we carried out Raman spectroscopy on each section. When HAP was abundant in such a way to observe positive von Kossa (black spots) even at 10x, then we were able to observe a Raman signal at ~960 cm^{-1} confirming the presence of HAP (please see top panel of **Figure 2**). However, the lower amount of HAP (hence, lower number or area of positive von Kossa) the more difficult it becomes to detect a reliable Raman signal (see middle panel of **Figure 2**) though samples without HAP clearly did not show a Raman shift at ~960 cm^{-1} (see bottom panel of **Figure 2**) In some sections, positive von Kossa is only detectible at 40x and may not be abundant throughout the sample making it nearly impossible to detect HAP via Raman spectroscopy. Therefore, we assume that tissue samples that scored positive for von Kossa and alizarin red S to be HAP positive. Based on these criteria, we obtained the results listed in **Table 1** and key metrics in **Figure 3**. From these results, HAP was more common among high grade serous ovarian cancer (HGSOC) than low grade serous ovarian cancer (LGSOC). These findings are consistent with findings by Wen *et al*. (12). While the sample size was small and no statistical significance was achieved between the groups in **Figure 3**, we observed a pattern that while samples (therefore, patients) with tumor extracellular HAP had nearly similar overall survival rate compared to those without tumor extracellular HAP, disease remission was more likely with those that were positive for HAP than those with negative HAP. This reinforces the need to dissolve tumor extracellular HAP for successful treatment of ovarian cancer.

Table 1. Extracellular HAP is more common in HGSOC than LGSOC. Analysis of ovarian tissue microarrays relative to the presence of tumor extracellular HAP.

Total number of samples analyzed	139
Total HGSOC	140
Total LGSOC	18
HGSOC with HAP	26
LGSOC with HAP	1
HGSOC with no HAP	114
LGSOC with no HAP	17
Number of samples unable to determine HAP status	7
HGSOC with HAP/total HGSOC (%)	19%
LGSOC with HAP/total LGSOC (%)	6%
Total number sensitive to platinum therapy	71
Total number with HAP sensitive to platinum therapy	14
Total number without HAP but sensitive to platinum therapy	57
% With HAP and platinum sensitivity	52%
% Without HAP but with platinum sensitivity	54%

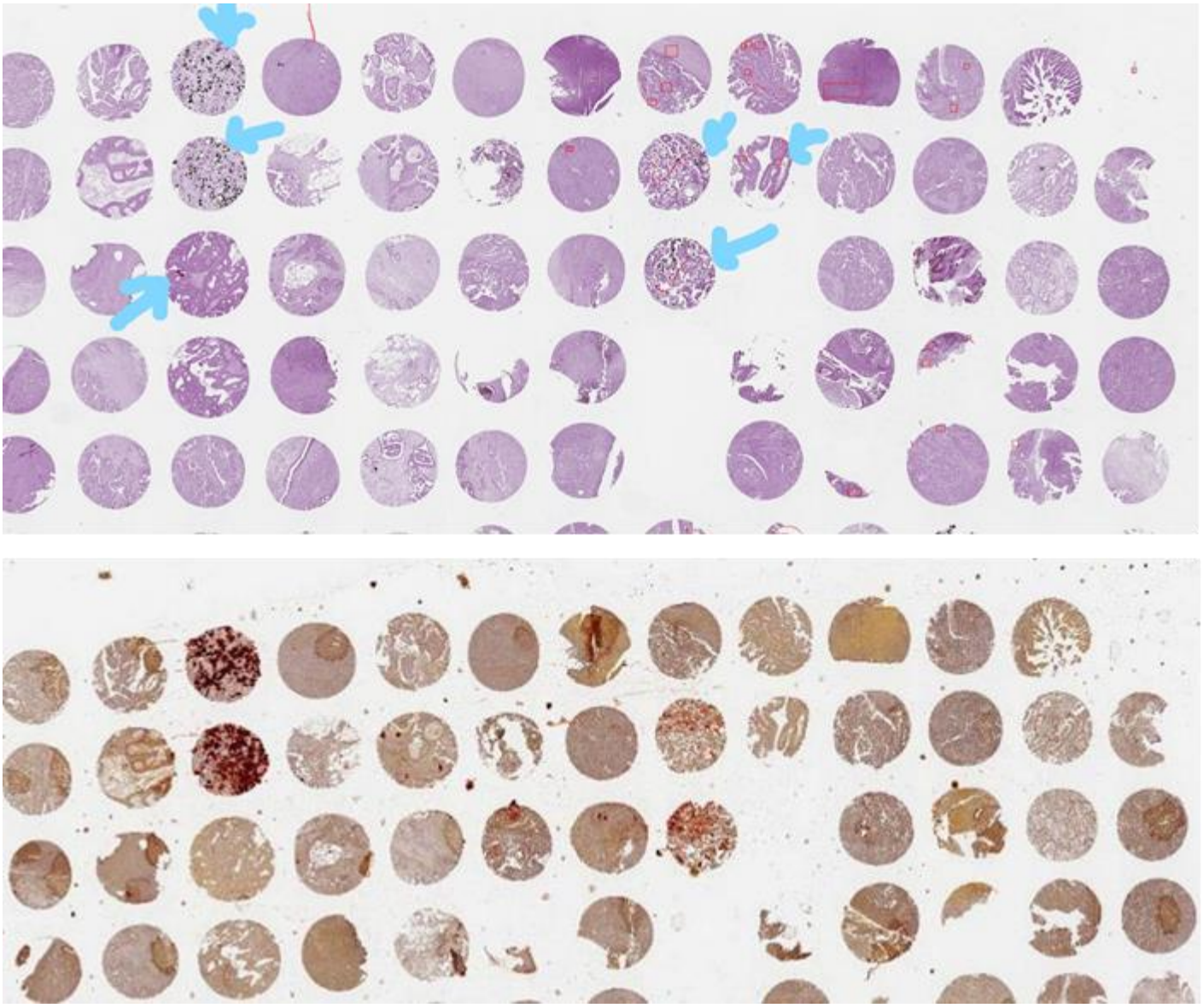

Figure 1. Stained tissue microarrays containing ovarian carcinomas. The TMAs were stained with von Kossa (Top) for phosphates and alizarin red S (bottom) for calcium. The dark spots are positive stains and the arrows point to some examples. If a section is positive for von Kossa and alizarin red S then that is a strong indication of the presence of tumor extracellular hydroxyapatite (HAP). If von Kossa is positive but alizarin red S is negative then further analysis is required (e.g. more samples of the same patient, Raman spectroscopy, stain for alkaline phosphates on the cell surface which helps in the production of HAP…. etc.). If alizarin red S is positive but von Kossa is negative, then that particular sample is most likely to be lacking HAP.

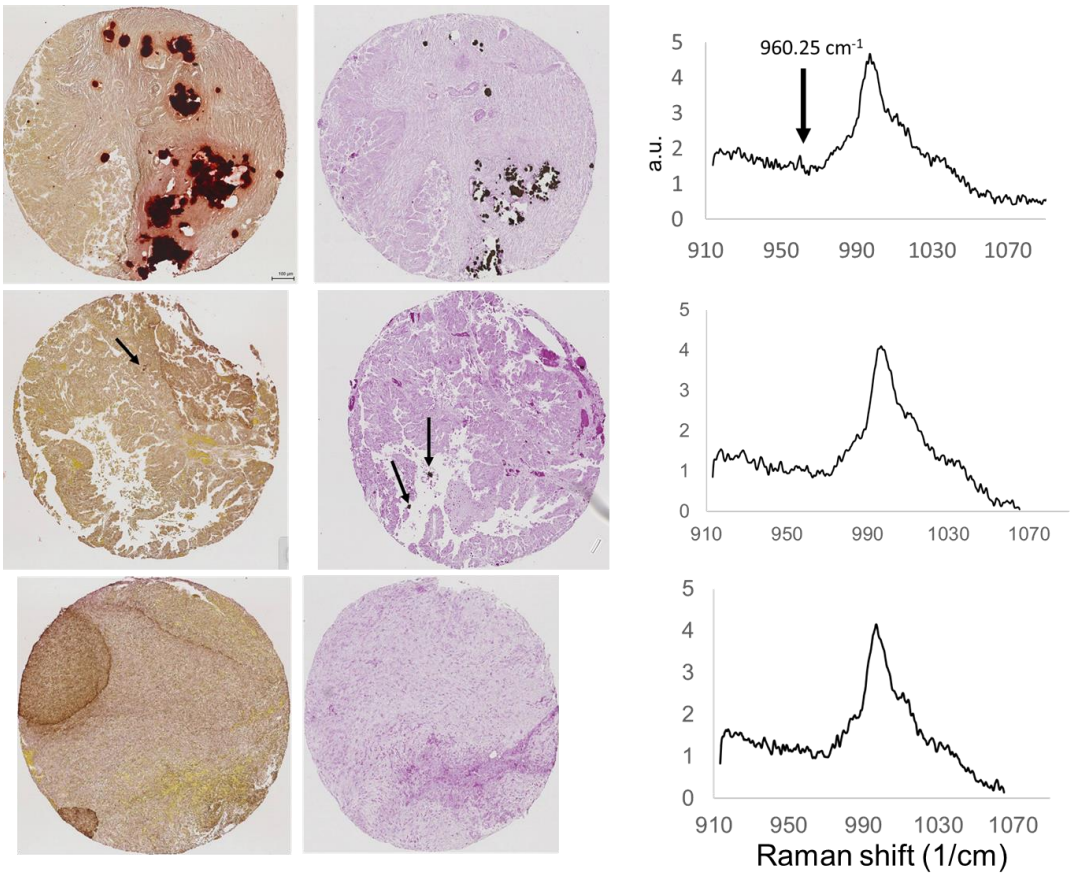

Figure 2: Detecting extracellular HAP in ovarian cancer TMAs. Sample images of ovarian tumor stained with Alizarin red S (left), von Kossa (middle) and imaged with Raman spectroscopy (right). Black spots in the alizarin red S stain indicate the presence of calcium. Black spots in the von Kossa stains indicate the presence of phosphates. Both stains may therefore, indicate the presence of calcium phosphates hydroxyapatite (HAP). A detectable Raman shift at ~960 cm^{-1} confirms the presence of HAP. However, as HAP becomes less abundant, a Raman shift at 960 cm^{-1} becomes more difficult to observe as in the middle panel. When a sample scores negative for both alizarin red S and von Kossa, then this sample is negative for HAP and can be easily confirmed with the complete absence of Raman shift at 960 cm^{-1} as in the bottom panel.

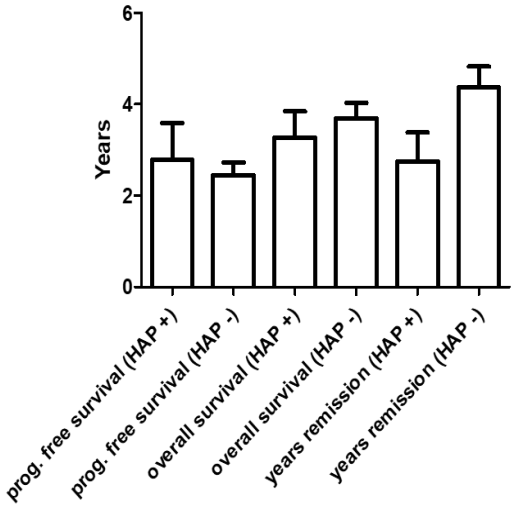

Figure 3. HAP may be correlated with lower number of years before ovarian cancer remission. Statistical analysis of ovarian tissue microarrays. While no statistical significance achieved, there is an apparent trend that overall survival and years with disease remission are lower in samples (and therefore, patients) with tumor extracellular HAP than those without.

To investigate the efficacy of NSPS on ovarian tumor, *in vitro*, ID8-luc cells were grown in normal culture media as described previously (13) and in osteogenic culture media similar to that described by Wen *et al*. (12). Briefly, normal medium consisted of 10% FBS-supplemented DMEM High-Glucose medium with 1% penicillin/streptomycin. Osteogenic medium consisted of normal medium + 50 μg/ml vitamin C, 10mM beta glycerin sodium phosphate + 10-7 M dexamethasone. When the cells were 50% confluent, they were treated in triplicates with 8 mmol of NSPS. Approximately 24 hour later, total and dead cells (those that absorb trypan blue) were counted in a hemocytometer. For negative control, we treated MCF10a normal breast cells, which are known to be absent of HAP (3), with 8 mmol of NSPS. Additionally, we used a micro-pH electrode to measure changes in pH immediately following application of NSPS to the cell cultures and 18 hours later before removing the media for counting. While we were able to observe a pattern of higher pH in the ID8 media compared to that of MCF10a and normal media, the pH measurements were not reliable and constantly fluctuating with a minimum of 7.5 at any time in the ID8 cells and a maximum of 7.42 at any time in the MCF10a and the control wells (wells containing ID8 but not treated with NSPS) since all cultured media used here were buffered with HEPES. However, since pH is a logarithmic scale, the difference between 7.5 and 7.42 is considerable. While we are working on verifying the ID8 cells cultured in the osteogenic media contains more HAP compared to those grown in normal media as expected and described by Wen *et al*. (12), the dead to total cell ratios were significantly higher ($p<0.05$) for the cells grown in the osteogenic medium compared to those grown in the normal medium and controls (please see **Figure 4**). Taken altogether, this supports the hypothesis that NSPS acts on tumor extracellular HAP resulting in acute alkalosis leading to tumor cell death. We are planning to repeat these studies on media that do not contain any kind of buffer to accurately evaluate changes in pH.

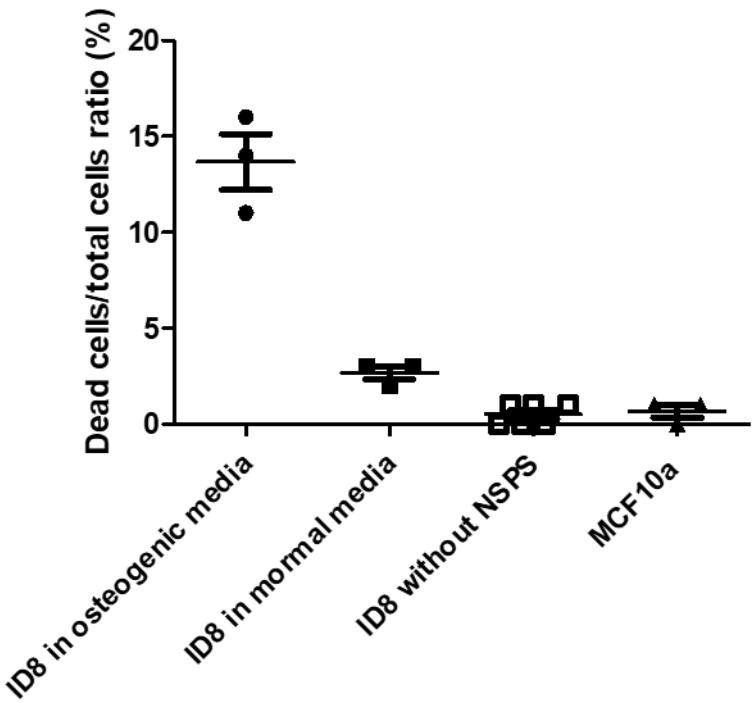

Figure 4. NSPS treatment leads to death of tumor cells containing HAP. ID8 cells were grown in normal or osteogenic media (to increase extracellular HAP) and normal breast cells, MCF10a, were treated with 8 mmol of NSPS and counted 18 hours later.

To demonstrate that tumor extracellular HAP is a viable candidate imaging biomarker for detecting ovarian tumor burden we imaged groups of mice bearing luciferase-tagged ID8 ovarian cells (ID8-Luc), a well-established murine model of HGSOC (13-15). Since the ID8 cells were luciferase-tagged, we injected the mice with luciferin and imaged them in a bioluminescence optical scanner. The bioluminescence images (BLI's) were used to detect tumors and quantified to assess tumor burden. Tumor burden was detected with ^{18}F-NaF PET (see Figure **5a**). As HAP is also present in bone and due to the large surface area of bone, bone uptake of ^{18}F-NaF and ^{99m}Tc-MDP was ~9 times higher than tumor uptake. Therefore, the bone signal appears saturated in

Figures 5 a&b. Due to the entrapment of ^{99m}Tc-MDP in the liver and the spatial resolution of our SPECT scanner (>1.2 mm), it was difficult to accurately detect tumor burden in the mice using ^{99m}Tc-MDP SPECT (see **Figure 5b**) especially since the tumors are generally close and/or on the peritoneal walls in front of the liver in the mouse models used here. However, in the clinic this may not be a problem since the liver and peritoneal cavity are generally on the order of many centimeters away from each other in adult females. Tumor burden was confirmed with BLI images (**Figure 5c**) and pathology (**Figure 5d**) indicating the tumor extracellular HAP may be a suitable imaging biomarker for detecting ovarian tumor burden using HAP-binding radioligands.

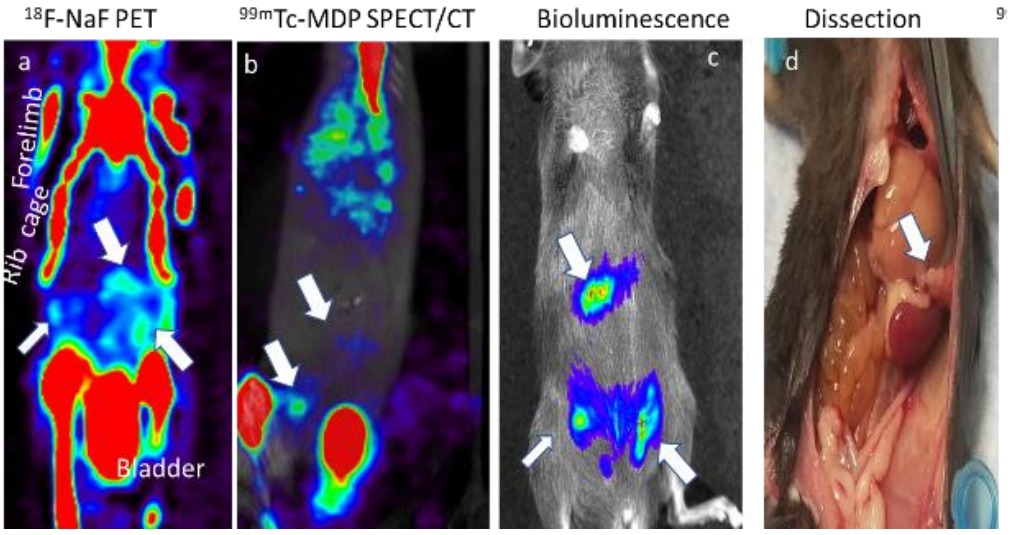

Figure 5. Tumor extracellular HAP as an imaging biomarker. (a) Mouse bearing peritoneal ID8-lucerase-taged tumors imaged with ^{18}F-NaF PET. White arrow points to tumor. Bone signal appears saturated as bone HAP uptake is ~9 times greater than that of tumor-extracellular HAP. (b) Same mouse imaged with ^{99m}Tc-MDP. Not only is there high uptake of the radiotracer in the bone, but the ^{99m}Tc-MDP is also trapped in the liver due to the presence of minerals. (c) Bioluminescence image of the same mouse using luciferin. (d) Pathology image of the same mouse.

To investigate the efficacy of NSPS, *in vivo*, we imaged mice with peritoneal ID8-luc tumors with ^{18}F-NaF PET and ^{18}F-FDG (for metabolism) PET at baseline and withing 48 hours hours following a bolus intraperitoneal administration of 100 mg/kg NSPS. A CT image of the mice was first obtained for anatomical co-registration (see **Figure 6a**). We measured significant decreases ($p<005$) in both ^{18}F-NaF (compare **Figures 6 b & C**) and in ^{18}F-FDG retention (compare **Figures 6 D & E**) in the peritoneal tumors following NSPS treatment reflecting reduction in tumor extracellular HAP and reduction and/or loss of tumor metabolic activity. It is unclear whether NSPS treatment results in the shutdown of tumor metabolism or whether there is a switch in metabolic pathways but would be worth investigating in future grant applications.At the end of imaging, the mice were euthanized and the abdominal wall containing peritoneal tumors were harvested and stained with Ki 67, caspase 3, CD8 and CD11b for T cell and macrophage infiltration (see **Figure 7**). The Ki 67 and caspase 3 stained slides were quantified as positive area percentage of the total tumor area using Image J (imagej.nih.gov) as displayed in **Table 2** and statistically analyzed using a non-paired t-test in Graphpad Prism V5. Notable observations from these preliminary histological analyses include: **(i)** positive Ki 67 was detected only along the circumference of the tumors in the NSPS treated mice while positive Ki 67 was detected throughout the tumors of the control mice. Percent positive Ki 67 area relative to tumor area was significantly higher in the tumors of the control mice vs that of the NSPS treated mice (**Table 2**). **(ii)** Opposite to Ki 67 findings, widespread positive caspase 3 was detected throughout the tumors from the NSPS-treated mice and significantly less or absent in the tumors of the control mice (see **Figure 7** and **Table 2**). **(iii)** positive CD8 cells were detected throughout the tumors of the NSPS treated mice indicating increased infiltration of cytotoxic T cells; a result that supports the argument of using NSPS to enhance tumor response to immunotherapy. On the other hand, the tumors of the control mice tested negative for CD8. However, both NSPS treated and control mice tested low positivity for CD11b. Thus, there may be more efficient infiltration of myeloid cells into the tumors following NSPS treatment. **(iv)** While not statistically significant in this pilot study, likely due to the small sample size, the size

of the peritoneal tumors from the NSPS-treated mice was on average ~60% smaller than the average tumor size of the control mice (visually compare tumor sizes in **Figure 7** and see **Table 2**). **(v)** Tumor cells could also be seen along the peritoneal walls (perhaps indicating the continuing seeding of new tumors) in both NSPS-treated and control mice. However positive Ki67 staining (proliferation) was observed along the peritoneal walls from the control mice with less so along those from the NSPS-treated mice. Taken together, the evidence is consistent with dissolution of tumor extracellular HAP having a significant inhibitory effect on ovarian tumor metabolism and proliferation leading to tumor cell death.

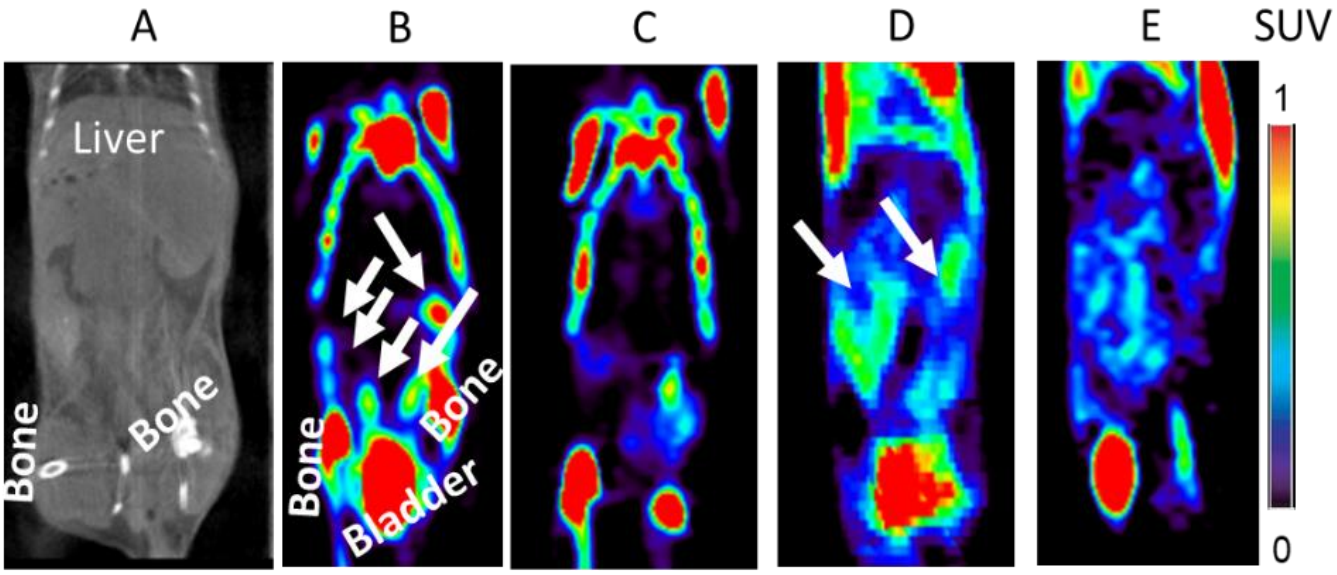

Figure 6. Treatment of mouse model of ovarian cancer with NSPS. (A) CT of a mouse bearing peritoneal ID8 tumors. (B) ^{18}F-NaF PET image of the same mouse at baseline. White arrows point to tumors. Radiotracer concentration in the peritoneal cavity and bone were 0.21 and 3.46 SUV, respectively. This is why the bone signal appears saturated. In the image. (C) ^{18}F-NaF PET image of the same mouse within 72 hours post NSPS treatment. Radiotracer concentration in the peritoneal cavity and bone were 0.11 and 3.65 SUV, respectively. (D) ^{18}F-FDG PET of the same mouse at baseline (before treatment). FDG concentration in the peritoneal cavity was 0.35 SUV (E) ^{18}F-FDG PET of the same mouse within 24 hours post NSPS treatment. FDG concentration in the peritoneal cavity was 0.05 SUV.

Table 2. NSPS induces HGSC apoptosis. TPS scores of IHC of ID8 peritoneal tumors harvested from mice treated with either NSPS or PBS (controls).

Treatment	% Area positive for Ki67	% Area positive for caspase 3	Area (μm^2) x 10^3
NSPS (n = 3)	1.05±0.39¥	17.42±2.14	4.21±1.61
PBS (n = 3)	3.02±0.33	7.73±3.86	7.03±2.37
p value	0.0026	0.0191	0.1637

¥ Values are displayed as mean ± STD.

As HAP is absent in normal soft tissue, no adverse effects of NSPS were observed. And while HAP is present on the surface of the bone, lack of vascularization combined with large skeletal surface area, crystalized (compact) formation of the bone HAP matrices, and continuous bone remodeling (16) make it difficult to dissolve. By contrast, tumor extracellular HAP are loosely scattered and not yet crystalized making it easier to dissolve. We did not measure changes in ^{18}F-NaF uptake in skeletal bone after NSPS treatment compared to that prior to treatment. Our next step is to extend the imaging protocol to several weeks following NSPS for efficacy and toxicity evaluation of NSPS.

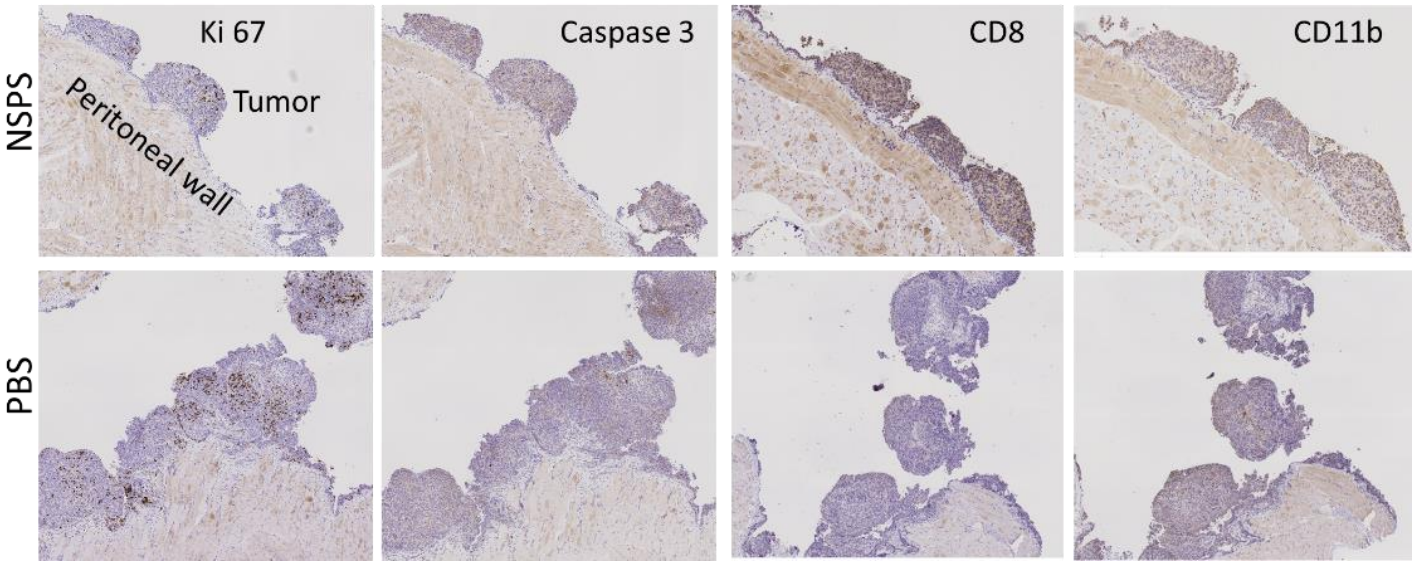

Figure 7. NSPS induces apoptosis and cytotoxic T cell infiltration in ovarian tumors. Sections of peritoneal walls containing ID8 tumors harvested from mice that were treated with NSPS (**top panel**) or vehicle PBS (**bottom panel**). Ki 67 for proliferation (dark spots), caspase 3 for apoptosis (brown regions within the tumors), CD8 for cytotoxic T cell infiltration (brown spots), CD11b for macrophage invasion (brown spots). See **Table 2.**

To investigate whether ^{18}F-NaF PET can track treatment progress of ovarian cancer via detecting changes in tumor-extracellular HAP, we imaged mice bearing peritoneal ID8-luc tumors weekly starting at 2 weeks post tumor cell injection. Then the mice were treated weekly with either PBS (controls) or cisplatin chemotherapy or treated once with NSPS. All mice were fasted the night before imaging. Three dimensional regions-of-interest (ROIs) were drawn around the peritoneal cavity in the PET images and ^{18}F-NaF retention was estimated for each week and time-activity curves (TACs) were established over the entire duration of the study for each group of mice (please see **Figure 8**). In the control, PBS treated mice (Group 1; n =3), we measured an increase in ^{18}F-NaF uptake in the tumors during tumor progression indicating an increase in tumor extracellular HAP (see **Figure 8**). Following cisplatin (Group 2; n = 3) we measured a reduction pattern in ^{18}F-NaF retention in the tumors of the treated mice indicating a reduction in tumor extracellular HAP. Additionally, we measured a decrease in ^{18}F-NaF uptake in the mice that were treated weekly with cisplatin for 2 weeks then an increase in radiotracer uptake within 2 weeks of switching to PBS (Group 3; n = 2) indicating tumor

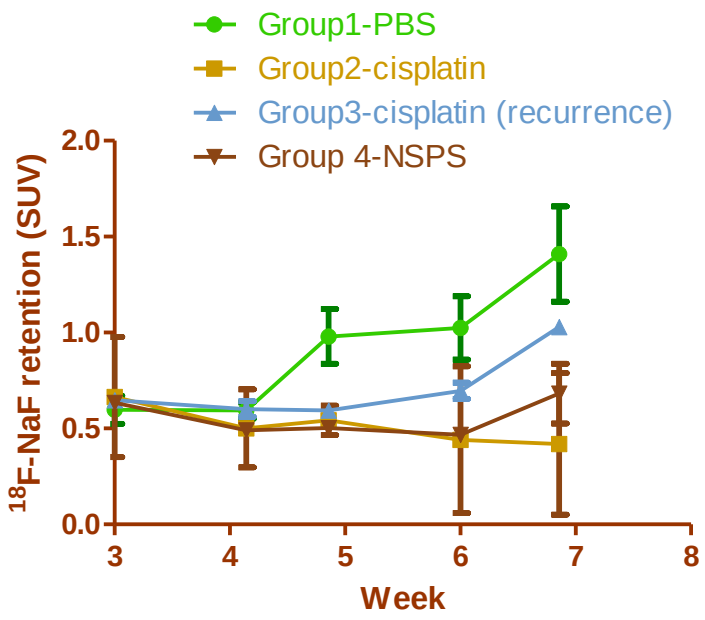

Figure 8. Tumor extracellular HAP is an imaging biomarker for tracking treatment progress. Time-activity curves (mean activity ± SD) of groups of mice injected i.p. with ID8-kuc tumors and imaged with ^{18}F-NaF PET three weeks later and weekly thereafter. At 4 weeks, the the mice were treated with weekly PBS (**group 1**; controls), 2 mg/kg cisplatin (**group 2**), 2 mg/kg cisplatin for 2 weeks then switched to weekly PBS (**group 3**; recurrence) or one time (not weekly) 100 mg/kg of NSPS (**group 4**). Tumor burden was assessed from retention of ^{18}F-NaF within the (peritoneal cavity). SUV: standard uptake value (normalized to dose and weight)

recurrence (see **Figure 8**). Therefore, we were able to track tumor extracellular HAP and tumor progression in the controls. The mice that were treated one time with NSPS demonstrated a trend similar to that of mice treated weekly with 2 mg/kg cisplatin as shown in the TACs of **Figure 8**. However, by week 6 tumor recurrence or continued tumor growth was detected in the mice treated with NSPS but not in the mice treated with weekly cisplatin. While NSPS may have resulted in the apparent inhibition of peritoneal metastases, this inhibition was not permanent and/or smaller tumors with little to no extracellular HAP my have been present during NSPS treatment and therefore, were not impacted by NSPS. Robey *et al*. have shown that bicarbonate, which increase whole body and tumor pH, inhibits spontaneous metastasis in breast and ovarian cancer models. In any case, these results indicate that periodic NSPS treatment, e.g. weekly, may be necessary for the effective treatment of HGSOC.

NSPS survival study. When a significant ID8-luc peritoneal tumor burden was detected by BLI (as defined by a BLI signal of > 1.5 x 10^6 radians/sec) with at least 3 distinct tumors clusters observed in the BLI, the equivalent of week 5 (post ID8-luc cell injections) in **Figure 8**, the mice (average weight = 20 ± 1 g) received one of the following treatments: (i) a bolus injection of 6.7 mg/kg NSPS (n = 5) one time (experimental group); (ii) weekly injections of 5 mg/kg Cisplatin (model of positive efficacy; n = 4); or (iii) bolus injection of PBS (controls; n = 4). **End point:** when any mouse (in any group) reached 24 g and abdominal bloating due to peritoneal ascites buildup was apparent, the mice were euthanized. Kaplan-Meier survival analysis was carried out on the data with the criteria that censored = 1 if the mice reached end point and 0 otherwise. Though the sample number was small, a log-rank (Mental-Cox) test yielded a statistically significant difference between all groups (p = 0.0016; df =2, chi^2 = 12.84) with the median survival of 4.64 and 2.98 weeks for the NSPS and PBS treated mice, respectively (please see **Figure 9**). With a limited time study, the median survival for the cisplatin treated mice could not be determined since none of the mice in that group reached the end point criteria. Comparison between the NSPS treated and the control group alone also showed a statistically significant difference in survival with p = 0.004 (df =1; chi^2 = 8.29). Thus, a single day of treatment with NSPS improved the survival of mice with ovarian cancer by >47%. This efficacy study also further supports the absence of adverse effects of NSPS till at least 6 weeks post administration (see **Figure 9**).

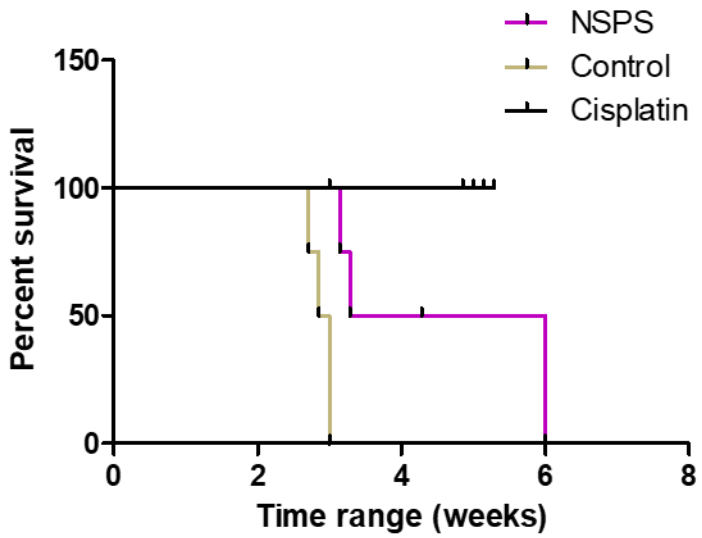

Figure 9. NSPS improves survival rate. Kaplan-Meier survival analysis of mice bearing peritoneal ID8-luc tumors and treated with 100 mg/kg o NSPS (n = 5), PBS (n = 4), or 5 mg/kg of platinum chemotherapy cisplatin (n = 4). P (df=2) = 0.0016. NSPS prolonged survival by over 47%.

C. Opportunities for training and professional development.

The studies carried out so far afforded important educational opportunities for PI including how to culture cells, how to maintain a colony of mice bearing peritoneal tumors, and grantsmanship. PI also participated in the March 2021, and March 2022 Society of Gynecology annual meeting. Though the meeting were virtual, the PI gained more knowledge about ovarian cancer and the strategies available or being developed for treating this disease.

D. Dissemination of results to communities of interest.

1. Preliminary results have been reported to our local ovarian cancer interest group (VOCAL) at Vanderbilt University Medical Center.
2. Poster presentation at the 2021-March and March 2022 annual meeting of the Society of Gynecologic Oncology

E. What do you plan to do during the next reporting period to accomplish the goals.

We had started a no cost extension period on this grant to complete the following goals:

1. We will continue to follow the plans outlined in our SOW.
2. We will complete statistical analysis of the TMAs to identify any potential correlations between ovarian cancer metrics and HAP.
3. We will attempt to establish pharmacokinetic parameters of NSPS.
4. We will increase our n to obtain statistically significant results of NSPS efficacy and treatment tracking.
5. Publish our results in peer review journals and present them at national meetings.

4. **Impact**

A. Impact on the development of the principal discipline

The treatment paradigm studied here can potentially be applied to other types of cancers that form solid tumors. The treatment paradigm also has the potential to treat other types of calcification-involved illnesses include arterial calcifications, liver and kidney calcification, neurodegenerative diseases that are due to the presence of excess neuro-extracellular calcium.

B. Impact on other disciplines

The treatment paradigm studied here can potentially be applied to other types of cancers that form solid tumors. The treatment paradigm also has the potential to treat other types of calcification-involved illnesses include arterial calcifications, liver and kidney calcification, neurodegenerative diseases that are due to the presence of excess neuro-extracellular calcium.

C. Impact on technology transfer

The proposed studies address two of the Ovarian Cancer Research Program (OCRP) objectives: (i) developing reliable diagnostic approaches and treatment; and (ii) providing the tools to study initiation, progression, treatment tracking, and recurrence of ovarian cancer.

There has been considerable progress in the management of patients with ovarian cancer, particularly those with high-grade serous ovarian carcinoma (HGSOC). While treatment now builds on the well-established backbone of surgery and paclitaxel/platinum-based chemotherapy (17) with surgery being carried out upon diagnosis or after neo-adjuvant chemotherapy (NACT), in a significant number of patients, the accurate assessment of initial tumor burden is challenging. Unfortunately, not infrequently patients are first selected for surgery when NACT (before surgery) would have been more appropriate. Further, in HGSOC patients, the assessment of tumor recurrence following surgery

and/therapy is less than optimal using current imaging modalities (CT, MRI and/or FDG-PET). The validation of more accurate assessment of tumor burden in HGSOC patients using 18F-NaF PET imaging as we propose would significantly enhance the clinical management of these patients.

Detection and early prediction of treatment response: imaging tumor extracellular HAP using 18F-NaF PET (already FDA approved) has not only shown to be able to detect peritoneal tumors with high specificity and signal-to-background ratio (SBR), but was also effective in assessing response to therapy by sensitively detecting changes in tumor extracellular HAP. This would allow patients to be spared multiple courses of expensive and toxic treatments and quickly move on to potentially more effective therapies.

There has been significant improvement in HGSOC patient survival using combination paclitaxel/platinum-based chemotherapy, particularly with the advent of second-line targeted therapies including bevacizumab and PARP inhibitors that have demonstrated progression-free survival benefits in certain clinically and molecularly defined subgroups. Despite this progress, about 70% of patients are likely to develop recurrent disease and require further treatment (17) with limited therapeutic options due to development of resistance to standard therapies. Likewise, current results with checkpoint inhibitors have been disappointing though strategies to enhance efficacy are being explored in current clinical trials. To address the limitations of current therapies, we successfully tested our novel NSPS therapeutic, designed to target HAP in the microenvironment of tumors, for treating HGSOC. Preliminary data demonstrates that application of NSPS lead to rapid tumor cell death. Our unique treatment strategy has the potential to significantly enhance the treatment options for HGSOC patients, particularly as second-line therapy.

D. Impact on society beyond science and technology

Nothing to report.

References:

1. Haka AS, Shafer-Peltier KE, Fitzmaurice M, Crowe J, Dasari RR, Feld MS. Identifying microcalcifications in benign and malignant breast lesions by probing differences in their chemical composition using Raman spectroscopy. Cancer research. 2002;62(18):5375-80. Epub 2002/09/18. PubMed PMID: 12235010.
2. Baker R, Rogers KD, Shepard N, Stone N. New relationships between breast microcalcifications and cancer. Br J Cancer. 2010;103(7):1034-9.
3. Cox RF, Hernandez-Santana A, Ramdass S, McMahon G, Harmey JH, Morgan MP. Microcalcifications in breast cancer: novel insights into the molecular mechanism and functional consequence of mammary mineralisation. Br J Cancer. 2012;106(3):525-37.
4. Morgan MP, Cooke MM, McCarthy GM. Microcalcifications associated with breast cancer: an epiphenomenon or biologically significant feature of selected tumors? Journal of mammary gland biology and neoplasia. 2005;10(2):181-7. Epub 2005/07/19. doi: 10.1007/s10911-005-5400-6. PubMed PMID: 16025224.
5. Frappart L, Boudeulle M, Boumendil J, Lin HC, Martinon I, Palayer C, Mallet-Guy Y, Raudrant D, Bremond A, Rochet Y, Feroldi J. Structure and composition of microcalcifications in benign and malignant lesions of the breast: study by light microscopy, transmission and scanning electron microscopy, microprobe analysis, and X-ray diffraction. Human pathology. 1984;15(9):880-9. Epub 1984/09/01. PubMed PMID: 6469237.
6. Radi MJ. Calcium oxalate crystals in breast biopsies. An overlooked form of microcalcification associated with benign breast disease. Arch Pathol Lab Med. 1989;113(12):1367-9. Epub 1989/12/01. PubMed PMID: 2589947.
7. Morgan MP, Cooke MM, Christopherson PA, Westfall PR, McCarthy GM. Calcium hydroxyapatite promotes mitogenesis and matrix metalloproteinase expression in human breast cancer cell lines. Molecular carcinogenesis. 2001;32(3):111-7. Epub 2001/12/18. PubMed PMID: 11746823.
8. Muttarak M, Kongmebhol P, Sukhamwang N. Breast calcifications: which are malignant? Singapore medical journal. 2009;50(9):907-13; quiz 14. Epub 2009/09/30. PubMed PMID: 19787181.
9. Holme TC, Reis MM, Thompson A, Robertson A, Parham D, Hickman P, Preece PE. Is mammographic microcalcification of biological significance? European journal of surgical oncology : the journal of the European Society of Surgical Oncology and the British Association of Surgical Oncology. 1993;19(3):250-3. Epub 1993/06/01. PubMed PMID: 8390947.
10. Wilson GH, 3rd, Gore JC, Yankeelov TE, Barnes S, Peterson TE, True JM, Shokouhi S, McIntyre JO, Sanders M, Abramson V, Ngyuen TQ, Mahadevan-Jansen A, Tantawy MN. An Approach to Breast Cancer Diagnosis via PET Imaging of Microcalcifications Using 18F-NaF. J Nucl Med. 2014. Epub 2014/05/17. doi: 10.2967/jnumed.114.139170. PubMed PMID: 24833491.

11. Felix DD, Gore JC, Yankeelov TE, Peterson TE, Barnes S, Whisenant J, Weis J, Shoukouhi S, Virostko J, Nickels M, McIntyre JO, Sanders M, Abramson V, Tantawy MN. Detection of breast cancer microcalcification using (99m)Tc-MDP SPECT or Osteosense 750EX FMT imaging. Nucl Med Biol. 2015;42(3):269-73. Epub 2014/12/24. doi: 10.1016/j.nucmedbio.2014.11.010. PubMed PMID: 25533764; PMCID: 4889014.
12. Wen J, Zhao Z, Huang L, Li L, Li J, Zeng Y, Wu J, Miao Y. Switch of the ovarian cancer cell to a calcifying phenotype in the calcification of ovarian cancer. Journal of Cancer. 2018;9(6):1006-16. Epub 2018/03/28. doi: 10.7150/jca.22932. PubMed PMID: 29581780; PMCID: 5868168.
13. Wilson AJ, Barham W, Saskowski J, Tikhomirov O, Chen L, Lee HJ, Yull F, Khabele D. Tracking NF-kappaB activity in tumor cells during ovarian cancer progression in a syngeneic mouse model. Journal of ovarian research. 2013;6(1):63. Epub 2013/09/12. doi: 10.1186/1757-2215-6-63. PubMed PMID: 24020521; PMCID: 3846584.
14. Roby KF, Taylor CC, Sweetwood JP, Cheng Y, Pace JL, Tawfik O, Persons DL, Smith PG, Terranova PF. Development of a syngeneic mouse model for events related to ovarian cancer. Carcinogenesis. 2000;21(4):585-91. Epub 2000/04/07. PubMed PMID: 10753190.
15. Janat-Amsbury MM, Yockman JW, Anderson ML, Kieback DG, Kim SW. Combination of local, non-viral IL12 gene therapy and systemic paclitaxel chemotherapy in a syngeneic ID8 mouse model for human ovarian cancer. Anticancer research. 2006;26(5A):3223-8. Epub 2006/11/11. PubMed PMID: 17094433.
16. Clarke B. Normal bone anatomy and physiology. Clinical journal of the American Society of Nephrology : CJASN. 2008;3 Suppl 3:S131-9. Epub 2008/11/15. doi: 10.2215/CJN.04151206. PubMed PMID: 18988698; PMCID: 3152283.
17. Mahmood RD, Morgan RD, Edmondson RJ, Clamp AR, Jayson GC. First-Line Management of Advanced High-Grade Serous Ovarian Cancer. Curr Oncol Rep. 2020;22(6):64. Epub 2020/06/05. doi: 10.1007/s11912-020-00933-8. PubMed PMID: 32494876; PMCID: PMC7270049.
18. Tantawy M, Wilson A, Beeghly-Fadiel A, Yull F, Gore J, Alvarez R, Crispens M, McIntyre JO. Tumor extracellular hydroxyapatite: a potential biomarker for imaging ovarian cancer. Gynecologic oncology. 2021;162:S318. doi: https://doi.org/10.1016/S0090-8258(21)01255-5.
19. Tantawy MN, Crispens MA, Beeghly-Fadiel A, Yull F, Watkins JC, McIntyre JO, Alvarez RD, Gore JC, Wilson AJ. Ovarian tumor associated hydroxyapatite: A potential biomarker for predicting treatment outcome. Gynecologic oncology. 2020;159:158-9. doi: 10.1016/j.ygyno.2020.05.228.

5. Changes/problems

A. Changes in approach and reasons for change

While attempting to do LC/MS, we found that NSPS gets trapped in the column making readings of NSPS metabolism in tissue unreliable. To overcome this problem, we may just use mass spectroscopy to determine the abundance of NSPS in tissue at different time points or label NSPS with an isotope, e.g. ^{99m}TC and track NSPS metabolism in tissue directly via imaging over the course of 48 hours .

B. Changes that had a significant impact on expenditures

The PI was promoted to Research Associate Professor on Jan 1st, 2021. This promotion came with a significant increase in pay. Additionally, inflation has caused supply charges to increase significantly. During the no cost extension period, only the PI, Drs. McIntyre and Wilson, as well as PI's research assistant, will continue to receive %effort as all remaining work on this project requires these personnel only.

C. Significant changes in use or care of human subjects, vertebrate animals, biohazards, and/or select agents

Nothing to report.

6. Products

1. New technique developed for detecting ovarian cancer and treatment tracking using ^{18}F-NaF PET. This technique has potential for rapid translation to the clinic as ^{18}F-NaF is already FDA-approved.

2. The imaging parts of this work had been presented at annual meetings of the Society of Gynecological Oncology (18, 19).

3. We will use the results displayed above to send a letter of intent to apply for a DoD OCRP TEA expansion Investigator initiated award.

7. **Participants & other collaborating organizations**

Name	Mohammed N Tantawy
Role	PI
Nearest person months worked	4 months
Contribution to project	Dr. Tantawy is the PI on the project and overlooked all experimental details of the project from animal monitoring to imaging and image analysis

8. **Change in PI funding support**

Nothing to report

9. **Special reporting requirement.**
Nothing to report

10. **Appendices**

Society of gynecological oncology 2021 annual meeting accepted abstract for poster presentation:

Title: Tumor extracellular hydroxyapatite - A potential biomarker for imaging ovarian cancer

Authors: Mohammed N. Tantawy, Andrew J. Wilson, Alicia Beeghly-Fadiel, Fiona E. Yull, John C. Gore, Ronald D. Alvarez, Marta A. Crispens and J. Oliver McIntyre.

Abstract:

Objectives: Hydroxyapatite (HAP), $Ca_{10}(PO_4)_6OH_2$, is produced by some types of malignancies, including breast and ovarian cancer, and deposited in the tumor extracellular microenvironment. HAP has a chemical composition and pattern of deposition distinct from solid calcium deposits that are detectable by conventional CT imaging. We have shown that HAP-binding radiotracers such as FDA-approved ^{18}F-NaF can be used with PET imaging to detect breast tumors; in this context, detection of tumor-associated HAP exhibited high specificity and a high signal-to-background ratio (SBR) as HAP is absent in normal soft tissue. In ovarian cancer, conventional imaging modalities lack clear metrics for assessing tumor burden before and after surgical debulking and for assessing tumor response to therapy. This is mainly due to lack of specificity and/or low SBR ratio from standard imaging. To address this limitation, and to determine whether tumor extracellular HAP could be an effective imaging biomarker for assessing peritoneal tumor burden using ^{18}F-NaF PET, we performed evaluative studies using a well-established synergic mouse model of ovarian cancer progression.

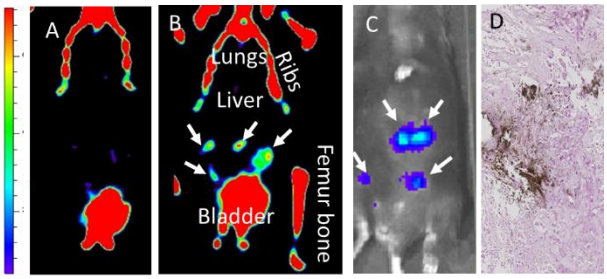

Figure A1. ^{18}F-NaF PET imaging of mouse model of ovarian cancer. (A) ^{18}F-NaF PET images of a normal healthy C57Bl/6 mouse. Total abdominal radiotracer concentration (Tot ARC) = 0.36 ± 0.08 microCi (n = 8, mean ± STD). **(B)** Mouse injected with ID8-luc ovarian tumors and imaged at 4 weeks with ^{18}F-NaF PET. Since normal soft tissue lacks HAP, the HAP-containing tumors are detected with high specificity. Tot ARC = 1.22 ± 0.18 μCi (n = 9). Total bone uptake of $^{18}F^-$ was 11.4 ± 3.0 μCi. **(C)** Luciferase bioluminescence imaging of the same mouse in B. Tumor distribution appears similar to the ^{18}F-NaF PET images. **(D)** A section of the one of the ID8 peritoneal tumors stained with von Kossa. The red/black spots are positive stain for calcium.

Methods: Female C57Bl/6 mice received intraperitoneal injection of ID8 mouse ovarian tumor cells that constitutively express a luciferase reporter (ID8-luc). After four weeks, bioluminescence imaging (BLI) was used to assess tumor burden and the mice were injected with ~11 MBq/0.1 mL of ^{18}F-NaF and imaged 60 min later for 20 min in a microPET/CT. HAP expression in harvested mouse tumors was determined by von Kossa and alizarin red S histological staining and confirmed by Ramen spectroscopy. HAP expression was similarly assessed using a clinically annotated tissue microarray (TMA) of patient samples from the Vanderbilt University Medical Center (VUMC) Tissue Repository for Ovarian Cancer (TROC).

Results: Among 117 cases from the VUMC TROC, HAP staining was more common among serous than non-serous and among late stage than early stage patients. We then confirmed HAP as a viable imaging target in ovarian tumors in the ID8-luc syngeneic model. Due to the absence of HAP in normal soft tissue (**Fig A1.A)**, peritoneal ovarian tumors were detected with high specificity and SBR (**Fig A1.B**) using ^{18}F-NaF PET which correlated well with BLI (**Fig A1.C**) and pathology. HAP presence was confirmed via histology including von Kossa (**Fig A1.D)** and alizarin red S staining and via Raman spectroscopy (not shown). As expected, bone uptake of ^{18}F-NaF was ~ 9 time greater than tumor uptake due to high HAP density and large surface area of bone. Therefore, the bone signal appears saturated in the images.

Conclusion: We show that imaging the deposition of tumor extracellular HAP may be an effective alternative tool for detecting ovarian tumors, particularly in late-stage serous disease. HAP-targeting ligands may yield a metric of disease status distinct from that obtained by conventional CT-based imaging of calcium deposits. Improvements in the clinical monitoring of tumor burden before and after surgical debulking and patient response to therapy has the potential to benefit women diagnosed with this devastating disease.

Poster:

SGO 2021 VIRTUAL ANNUAL MEETING ON WOMEN'S CANCER®

Tumor extracellular hydroxyapatite - A potential biomarker for imaging ovarian cancer

Mohammed N. Tantawy[1,2], Andrew J. Wilson3, Alicia Beeghly-Fadiel[4], Fiona E. Yull[5], John C. Gore[1,2], Ronald D. Alvarez[3], Marta A. Crispens[3,6] and J. Oliver McIntyre[1,2]

[1]Department of Radiology and Radiological Sciences, [2]Vanderbilt University Institute of Imaging Science, [3]Department of Obstetrics and Gynecology, [4]Division of Epidemiology, [5]Pharmacology, [6]Division of Gynecologic Oncology; Vanderbilt Medical Center and Vanderbilt University; Nashville TN

Society of Gynecologic Oncology

Introduction

- Carbonated calcium hydroxyapatite (HAP), $Ca_{10}(PO_4)_6OH_2$ type II microcalcifications [1]:
  - Major component of bone
  - Produced by and deposited in the extracellular matrix of some malignancies [1] including ovarian cancer [2]:
    - ALP on surface of cells hydrolyses βG → glycerol + Pi
    - Pi + Ca in the cell → HAP - HAP is deposited in the extracellular matrix contributing to the structure of the tumor microenvironment in a number of solid tumors.

Goals, Methods, & Results

1-Investigate correlations (if any) between tumor extracellular HAP and ovarian cancer in clinical samples: 117 cases from the Vanderbilt University Medical Center (VUMC) Tissue Repository for Ovarian Cancer (TROC) were stained with von Kossa and alizarin red S and also analyzed using Raman microspectroscopy.

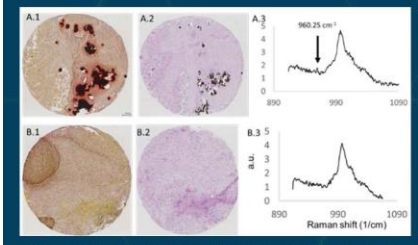

(**A.1**) A sample from a patient with HGSOC stained with alizarin red S (for calcium) and (**A.2**) von Kossa (for phosphates). Dark spots indicate positive stains. (**A.3**) A Raman shift at ~960 cm^{-1}, characteristic of hydroxyapatite, was clearly detected despite silica interference from a glass slide (a large peak between 990 and 1040 cm^{-1} (13)). Taken together, this indicates the presence of extracellular HAP. (**B.1**) A sample from a patient with HGSOC but scored negative for alizarin red S and (**B.2**) von Kossa. (**B.3**) No Raman shift was detected at ~960 cm^{-1} indicating absence of extracellular HAP.

HAP staining was more common among serous than non-serous ovarian cancer (consistent with [2]) and among carcinomas from late stage than early stage patients.

2-Investigate tumor extracellular HAP as an *in vivo* imaging metric for tumor burden, distribution, and monitoring treatment response to therapy in the ID8 mouse model of HGSOC [3] using ^{18}F-NaF PET or ^{99m}Tc-MDP SPECT:

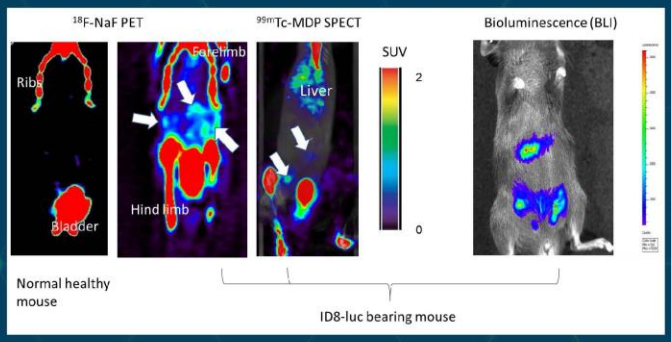

In vivo imaging & treatment schedule

^{18}F-NaF (FDA approved): 18 MBq (retro-orbital) → 1 hour uptake → 20 min PET (Inveon microPET, Siemens)

^{99m}Tc-MDP (FDA approved): 37 MBq (retro-orbital)→ 1 hour uptake → 20 min SPECT/CT (NanoSPECT/CT, Mediso)

Luciferin: 0.1 mL → BLI (IVIS, Perkin Elmer)

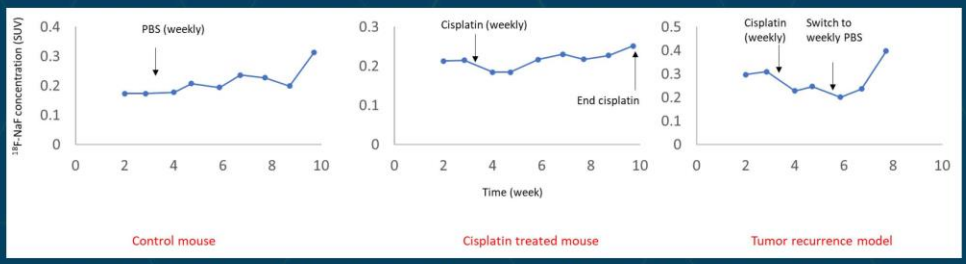

Typical uptake of ^{18}F-NaF in peritoneal cavity (lower abdomen) in ID8-luc tumor-bearing mice measured weekly after tumor establishment; mice were treated with cisplatin (or PBS control) as indicated.

Conclusion

- **^{18}F-NaF PET targeting tumor extracellular HAP→ detect peritoneal tumor burden with high specificity and contrast-to-background ratio as HAP is generally absent in normal soft tissue.**
- **^{18}F-NaF PET imaging appears to correlate with BLI but not ^{99m}Tc-MDP SPECT imaging that was confounded by liver uptake.**
- **Preliminary results suggest that ^{18}F-NaF PET imaging has potential for tracking: tumor progression, regression, recurrence, and early identification of tumor resistance to cisplatin chemotherapy**

References

1. Cox RF *et al*. Br J Cancer. 2012;106(3):525-37.
2. Wen J *et al*. Journal of Cancer. 2018;9(6):1006-16
3. Wilson AJ *et al*. Molecular cancer. 2015;14:192

Acknowledgement

This work was supported by DoD grant # W81XWH-20-1-0269. The Inveon microPET was funded by NIH 1S10 OD016245 and the IVIS was funded by 1S10 OD021804-01A1